

Concentric Symmetry

Filipi N. Silva¹, Cesar H. Comin^{1,*}, Thomas K. DM. Peron¹, Francisco A. Rodrigues²,
Cheng Ye³, Richard C. Wilson³, Edwin Hancock³, and Luciano da F. Costa¹

¹*Instituto de Física de São Carlos, Universidade de São Paulo, São Carlos, São Paulo, Brazil*

²*Departamento de Matemática Aplicada e Estatística,*

Instituto de Ciências Matemáticas e de Computação, Universidade de São Paulo,

Caixa Postal 668,13560-970 São Carlos, São Paulo, Brazil

³*Department of Computer Science, University of York, York, YO10 5GH, United Kingdom*

The quantification of symmetries in complex networks is typically done globally in terms of automorphisms. In this work we focus on local symmetries around nodes, which we call connectivity patterns. We develop two topological transformations that allow a concise characterization of the different types of symmetry appearing on networks and apply these concepts to six network models, namely the Erdős-Rényi, Barabási-Albert, random geometric graph, Waxman, Voronoi and rewired Voronoi models. Real-world networks, namely the scientific areas of Wikipedia, the world-wide airport network and the street networks of Oldenburg and San Joaquin, are also analyzed in terms of the proposed symmetry measurements. Several interesting results, including the high symmetry exhibited by the Erdős-Rényi model, are observed and discussed.

I. INTRODUCTION

The study of graph symmetry has its roots in algebraic graph theory [1–4]. In this context, symmetry is defined in terms of *automorphisms* and the *orbits* of the nodes in a given graph. More specifically, an automorphism of a graph G is a permutation of the vertex labels which preserves the label adjacency relation of the original graph. The orbit of a given vertex is the set of remaining vertices that share a label over the permutations in a automorphism group [1–4]. It is then assumed that a network is symmetric if it has at least one vertex label permutation such that the label adjacency remains unchanged. Otherwise, the network is considered to be asymmetric [1–5].

Despite the great amount of work devoted to the structural and dynamical characterization of complex networks, the study of symmetry has received less attention, including works such as [5–7]. In algebraic graph theory, the study of symmetry is focused on simple graphs. More recently, measurements based on automorphisms and orbits have been employed to analyse the structure of complex networks. For instance, Xiao et al. [5] applied the size of automorphisms groups [7] to quantify the symmetry of real-world complex networks, showing that the emergence of symmetry in such networks is a consequence of similar patterns of connectivity. Furthermore, in [5] the authors proposed a variation of the preferential-attachment mechanism in which new nodes are connected with probability proportional to the degree of previously existing nodes together with their local symmetry. Interestingly, the model was capable of reproducing the symmetry properties observed in real-world networks, reinforcing the hypothesis that similar linkage properties are crucial for the emergence of overall symmetry [5].

While symmetry measurements based on automor-

phisms typically apply to the whole graph, it is also possible to develop approaches aimed at quantifying symmetry locally, for instance using a given reference node. One of the first studies of local symmetry in complex networks was reported by Holme [6], where the so-called *degree-symmetry* of a node was proposed. Although this allowed the local symmetry to be quantified with respect to a reference node, occasional negative values can be obtained. Also, that measurement does not possess clear bounds, making the comparison of the symmetry of patterns with different structures less clear.

There are several reasons why to quantify the topological symmetry around specific nodes of a network. To begin with, the intrinsic way in which several networks, synthetic or real, are constructed, tends to imply a characteristic local symmetry. For instance, patterns in city networks should reflect the grid-like organization typically adopted in urban planning. On the other hand, the hubs in scale free networks could be expected to disrupt the local symmetry. Interestingly, such types of symmetries characteristic to different networks are also expected to impact the dynamics unfolding in the respective structure. For instance, highly symmetric patterns would be expected to promote a more uniform traffic flow in a city. Though the previously introduced [8] accessibility measurement has been found to provide valuable information about the local properties of the topology around a node (e.g. it can be used to define the borders of a network [9]), it is highly influenced by its degree, and therefore becomes related to many other degree-related measurements. Contrariwise, the value of the local symmetry should not be directly influenced by the degree of the reference node, which can be done by a suitable normalization.

Here, as in [6], we study local symmetry across the concentric levels of a reference node, where a concentric level is defined as the set of nodes having the same shortest path length to the reference node. However, our definition of symmetry is based on the accessibility of a

*Electronic address: chcomin@gmail.com

node [8, 10], which is also a concentric measurement. The accessibility of a node for a given concentric level is calculated from the transition probabilities of that node to the neighbors at that level. These transition probabilities are defined by the dynamics imposed on the network, such as self avoiding random walks or epidemic spreading. The accessibility of a node is high when the transition probabilities at that given concentric level tend to be uniform. The number of nodes in a concentric level is referred to as the number of reachable nodes. The accessibility of the concentric level attains its maximum value when all transition probabilities at that level are equal. In this case, the accessibility, or effective degree, of the reference node becomes equal to the number of reachable nodes, indicating that they can be optimally accessed. We combine a normalized version of accessibility with a variation of the random walk dynamics, referred to as the concentric random walk, to evaluate the symmetry of the concentric level of nodes in the network. This specific type of random walk is adopted in order to avoid transitions of moving agents to previous concentric levels, which would otherwise reduce the exploration of the remainder of the network. Two symmetry indices can be derived from this type of dynamics. The first is the *backbone symmetry*, in which the links inside a concentric level are eliminated (no transition between them). The second is the *merged symmetry*, in which these links assume cost zero in the transition. As such, these two indices provide complementary quantification of the local symmetry around a given node.

Complex networks have been defined as graphs with a topology that is more *irregular* than that in a uniformly random model such as Erdős-Rényi [11]. Formally, a graph is said to be regular[3] if all its nodes have the same degree, implying some level of uniformity and simplicity. However, it is known that the degree alone is not sufficient to completely specify a graph. So, the *complex* in complex networks actually refers to intricate distributions not only of degree, but also of other measurements, as discussed in [11]. In this context, the two measurements proposed in the current article can be understood not only as a quantification of node-centered symmetry, but also as a more robust evaluation of its regularity, and therefore *simplicity*, of the network. In other words, complex networks could be characterized and even defined as graphs possessing several nodes presenting high values of backbone and merged symmetry measurements.

This paper is organized as follows: Section II presents our modification of the accessibility measurement, which are used to define the backbone and merged symmetry measurements. Section III is devoted to the characterization of symmetry patterns emerging in random network models. The same analysis is performed for real-world networks in Section V. Finally, conclusions are presented in Section VI.

II. THE BACKBONE AND MERGED SYMMETRIES

The two symmetry measurements are defined here for each concentric level [12] $\Gamma_i^{(h)}$ of a given reference node i , where the concentric level is defined as the set of nodes that are at topological distance h from i . For example, the first concentric level is the set $\Gamma_i^{(1)}$ of neighbors of node i . The symmetries are calculated in terms of the transition probabilities of a *concentric random walk*. In this type of dynamics, the agent cannot return to the previous concentric level, which would be detrimental to the diffusion to more distant levels. For the same reason, i.e. to enhance the exploration of further levels, the edges between nodes belonging to a same concentric level should be treated differently. There are two ways to deal with these intra-level edges: (i) to remove them; and (ii) to join the nodes which they interconnect. This gives rise to two intermediate representations of the pattern. Therefore, the concentric random walk is specified with respect to these two structures, as explained in this section.

In this article, we define a *l-pattern* centered at reference node i as the subgraph of the original network containing the nodes at the l first concentric levels of i . In Figure 1(a) we show an example of a 2-pattern and indicate by dashed lines the concentric levels of the pattern. In Figure 1(b) we indicate by arrows the one-step transitions that the concentric random walk is allowed to move. In order to cover effectively the neighborhood of a node, in h steps the agents of the concentric random walk should be able to arrive at all nodes of the h -th concentric level. Since allowing a transition between edges connecting nodes of the same concentric levels would make the coverage less effective, such connections are treated in a special manner. In fact, we define two possibilities for the transition over these edges, the infinite-cost and the zero-cost transitions. In the former case, the walker can never go through an edge connecting nodes at the same concentric level. In the zero-cost case, the walker can move freely inside the concentric level, that is, going from one node to another does not count as an iteration of the dynamics. These two cases can be exactly represented by two transformations of the network topology. For the infinite-cost transition, it suffices to remove all connections within the same concentric level, as shown in Figure 1(c). We call the resulting network the *backbone pattern*. In the case of zero-cost transitions, connected nodes that are at the same concentric level are merged to form a single node, and the neighbors of the merged nodes are connected to the single node. Also, the number of connections made by the merged nodes with other concentric levels become the weight of the connection assigned to the new node. Figure 1(d) shows the network obtained from the pattern in Figure 1(a). We call the resulting network the *merged pattern*. For the backbone and merged patterns shown in Figure 1, we indicate by arrows all possible one-step transitions for the concentric random walk, as well as their respective probabilities.

In the remainder of this work, we will always use the terms backbone and merged to refer, respectively, to the infinite-cost and zero-cost transitions over edges within concentric levels.

The backbone and merged representations can provide complementary information about the topological symmetry of the neighborhood of a node, therefore we define a symmetry measurement for each representation, which we call *backbone symmetry* and *merged symmetry*, respectively. Both symmetries are obtained by treating the backbone and merged patterns as follows. We represent as $P^{(h)}(i \rightarrow j)$ the probability that a walker undergoing a concentric random walk goes from node i to node j in h steps. This allow us to define the following transition probabilities for nodes j belonging to the set $\Gamma_i^{(h)}$

$$P^{(h)}(i \rightarrow j|i \rightarrow k, \forall k \in \Gamma_i^{(h)}) = \frac{P^{(h)}(i \rightarrow j)}{\sum_{k \in \Gamma_i^{(h)}} P^{(h)}(i \rightarrow k)}, \quad (1)$$

This expression can be understood as the probability of the walker being at node j , given that it arrived at some node of the h -th concentric level of node i . For simplicity's sake, we henceforth replace $P^{(h)}(i \rightarrow j|i \rightarrow k, \forall k \in \Gamma_i^{(h)})$ by $P^{(h)}(i \rightarrow j|i \rightarrow \Gamma_i^{(h)})$. We then calculate the Shannon entropy of the transition probabilities as

$$\begin{aligned} H_i^{(h)} &= - \sum_{j \in \Gamma_i^{(h)}} P^{(h)}(i \rightarrow j|i \rightarrow \Gamma_i^{(h)}) \ln[P^{(h)}(i \rightarrow j|i \rightarrow \Gamma_i^{(h)})] \\ &= - \sum_{j \in \Gamma_i^{(h)}} \frac{P^{(h)}(i \rightarrow j)}{P^{(h)}(i \rightarrow \Gamma_i^{(h)})} \ln \left(\frac{P^{(h)}(i \rightarrow j)}{P^{(h)}(i \rightarrow \Gamma_i^{(h)})} \right). \end{aligned} \quad (2)$$

Now defining $\xi_i^{(h)}$ as the set of reachable nodes from node i , for walks of length h (i.e., $\xi_i^{(h)} = \{j|P^{(h)}(i \rightarrow j) > 0\}$), we calculate the respective symmetry measurement as

$$S_i^{(h)} = \frac{e^{H_i^{(h)}}}{|\xi_i^{(h)}|} \quad (3)$$

where $|X|$ is the cardinality of the set X . Therefore, to each node of the network the backbone and merged symmetry measurements, $\{Sb_i^{(h)}, Sm_i^{(h)}\}$, are assigned to the h -th concentric level of node i . We use the exponential of the entropy in order to have the number of reachable nodes as dimension [8], which is more intuitive and compatible with $|\xi_i^{(h)}|$. Observe that both measurements of symmetry are bounded between 0 and 1.

These measurements are illustrated in the following example. For the 2-pattern shown in Figure 2(a), we calculate the two symmetry measurements for node 0 with respect to the second concentric level. First, we create the backbone and merged patterns, as shown in Figures

2(b) and (c). The backbone pattern is the original network without the connections within the first concentric level. For the merged pattern, nodes 1,2,3 and 4 are merged into a single node, and this new node connects to all neighbors of the merged nodes. Since four connections between concentric levels were merged into a single one, the new connection between node 0 and the merged node has weight 4. For the backbone pattern, $\Gamma_0^{(2)} = \{5, 6, 7, 8\}$ and $\xi_0^{(2)} = \{5, 6, 7, 8\}$. Therefore, the entropy of the transition probabilities is calculated as

$$\begin{aligned} H_0^{(2)} &= - \sum_{j \in \Gamma_0^{(2)}} \frac{P^{(2)}(0 \rightarrow j)}{P^{(2)}(0 \rightarrow \Gamma_0^{(2)})} \ln \left(\frac{P^{(2)}(0 \rightarrow j)}{P^{(2)}(0 \rightarrow \Gamma_0^{(2)})} \right) \\ &= -4 \frac{1/4}{1} \ln \left(\frac{1/4}{1} \right) \\ &= \ln(4) \end{aligned}$$

The backbone symmetry is then given by

$$\begin{aligned} Sb_0^{(2)} &= \frac{e^{H_0^{(2)}}}{|\xi_0^{(2)}|} \\ &= \frac{4}{4} = 1. \end{aligned}$$

For the merged pattern, the calculation is analogous, but with the difference that the edge weights are incorporated into the transition probabilities. In this case, both measurements attain the maximum possible value, which is expected since the original pattern is symmetric.

In Figure 2(d) we provide another example where the neighborhood of the node is not perfectly symmetric. The respective backbone and merged patterns are shown in Figures 2(e) and (f). Note that a self-loop is added to node 3 of the backbone pattern. This is done because when the walker reaches node 3 it becomes trapped at that node. The probability of being at node 3 is not considered when calculating $H_0^{(2)}$, since only the transition probabilities to nodes at the second concentric level are relevant. Nevertheless, the self-loop is still necessary because node 3 is in the set of nodes reachable from node 0. Therefore, the nodes in the second concentric level are $\Gamma_0^{(2)} = \{5, 6, 7\}$ and the reachable nodes are $\xi_0^{(2)} = \{3, 5, 6, 7\}$. The remaining calculation is the same as above. For this case, the backbone symmetry is $Sb_0^{(2)} = 0.75$ and the merged symmetry is $Sm_0^{(2)} = 0.97$.

III. NETWORK MODELS

Let us start by characterizing the Erdős-Rényi (ER) model in terms of the backbone and merged symmetries $\{Sb_i^{(h)}, Sm_i^{(h)}\}$. In Figure 3 we show the scatterplots of $Sb_i^{(h)}$ as a function of $Sm_i^{(h)}$ for $h = 2$ and 3, together with some patterns with their corresponding symmetry values. For $h = 2$ (Figure 3 (a)) we see that there is high

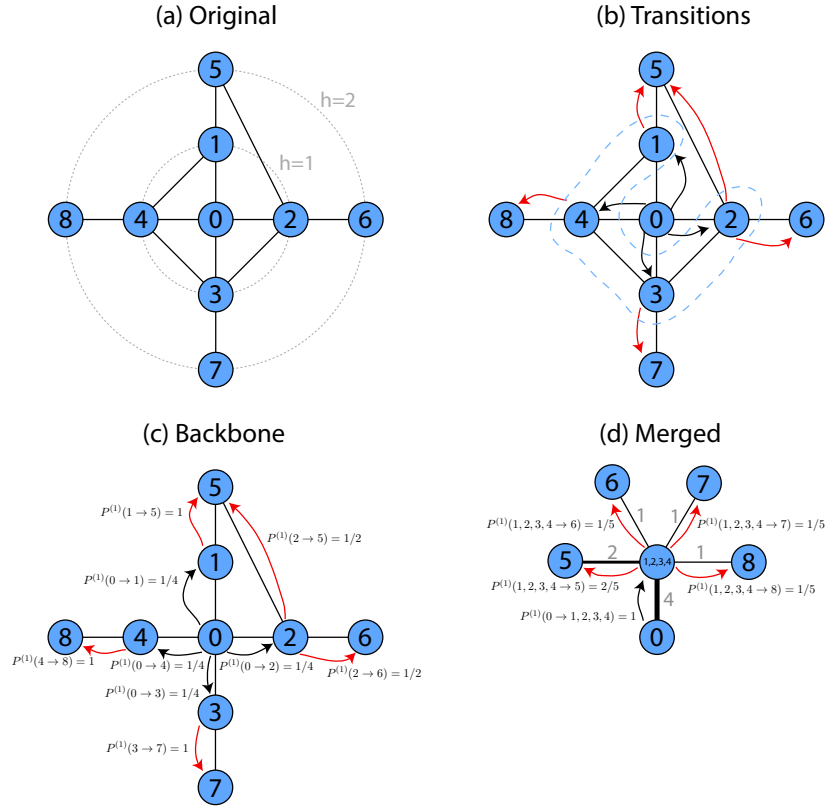


FIG. 1: Illustration of the concentric random walk dynamics. (a) Original 2-pattern considered, with concentric levels indicated by dashed lines. (b) One step transitions allowed for the random walk, indicated by arrows. Black and red arrows are for transitions departing from, respectively, the first and second concentric levels. Nodes inside the blue dashed line form a connected group inside the first concentric level. Treating the connections between these nodes as infinite-cost or zero-cost is equivalent to representing the original pattern as, respectively, the (c) backbone and (d) merged patterns.

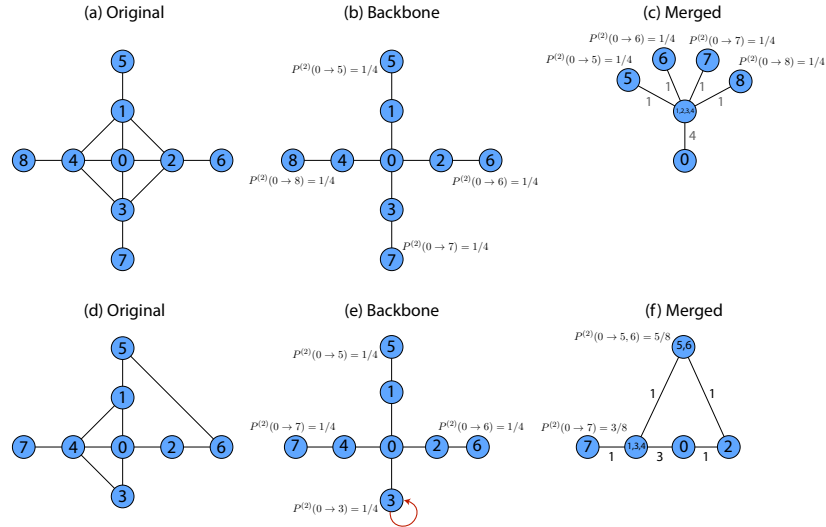


FIG. 2: (a) Initial 2-pattern and its respective (b) backbone and (c) merged transformation. (d) Another example with a different 2-pattern and the respective (e) backbone and (f) merged patterns.

density of subgraphs occurring for values of $Sb_i^{(2)}$ close to $Sm_i^{(2)}$, with a great homogeneity of observed patterns. Note, also, that most of these patterns are tree-like, i.e., without the presence of triangles. This pattern is frequently found in uncorrelated networks [13]. Therefore, for low values of h , the ER model yields highly symmetric patterns, essentially as a consequence of the aforementioned tree-like characteristic of the network.

The scenario changes as we increase the value of h . For $h = 3$ (Figure 3 (b)), the symmetry values are smaller than in the former case. This effect is stronger for the merged symmetry. This can be explained by the small-world characteristic of the ER model. Since these networks have average shortest path lengths of order $\ell \sim \ln N$, with a few steps all nodes can be reached (given that the networks contains only one connected component), becoming highly unlikely that a symmetric structure is obtained. Any eventual connection between the same level will not change the backbone symmetry, but will strongly impact on the merged symmetry. Since for larger h the probability of having a connection on the same level is larger, the merged symmetry values tend to decrease. Note in Figure 3 that patterns below the line $S_m^{(2)} = S_b^{(2)}$ often present a higher number of connections (see Figure 14).

Next we turn our analysis to spatial random graphs in order to study spatial effects on the symmetry of patterns. First we consider the random geometric graphs (GEO) whose nodes are connected if they are separated by distances smaller than a certain distance [14]. As we can see in Figure 4, the GEO network behaves similarly to the ER model, though with more accentuated decrease in the merged symmetry as we increase the value of h . Unlike the ER model, GEO networks do not have local tree-like structures, but rather a high number of triangles implied by connecting all nodes within a certain radius. The increase in the clustering coefficient leads, therefore, to more connections between nodes at the same concentric level, a fact that is reflected by the larger dispersion in the values of the merged symmetry for $h = 2$ in Figure 4(a). Moreover, for $h = 3$ (Figure 4(b)), we observe a striking difference between the GEO networks and the ER structures. Although perfectly symmetric patterns can still be observed, the symmetry of the merged patterns decrease significantly, suffering even more the effects of high clustering.

Another example of a spatial random graph, namely the Waxman model (WAX) [15, 16], is shown in Figure 5. Interestingly, both symmetries tend to be smaller than the values obtained for GEO. It is worth noting that there is a non-vanishing probability of observing long-distance connections in the WAX model, a fact that might explain the loss of backbone symmetry for larger values of h .

Voronoi networks [16–18] (VOR) are typically obtained from a given spatial distribution of nodes in a metric space, and pairs of nodes are interconnected whenever their Voronoi cells touch one another. Figure 6(a) illustrates the backbone and merged symmetries for $h = 3$,

as well as some representative patterns. Figure 6(b) presents analogue results obtained for a rewired Voronoi network (RVOR), obtained by randomly selecting links in the previous network and placing them between a randomly chosen pair of nodes (the rewiring probability is 0.001).

The Barabási-Albert (BA) model is our final example considering network models. We note in Figure 7 that the most symmetric patterns are those centered at nodes with smaller degree. On the other hand, hubs have lower values of merged symmetry, as high degrees tend to imply larger probability of reaching non-symmetric regions in the network.

It is also interesting to verify how the symmetry values correlate with the node degrees. We include in Appendix A scatterplots of the backbone and merged symmetries for the second, third and fourth concentric levels. We colored the symbols according to the degree of the reference node. For all models (shown in Figures 14, 15, 16, 17, 18 and 19), except BA, nodes with higher degrees tend to present lower symmetry values, specially for the merged symmetry. This happens because nodes with larger degrees commonly have more nodes at their initial concentric levels. Since it is less probable that patterns having a large number of nodes remains symmetric, such nodes have lower level of symmetry.

We also investigate the correlations between the symmetry measurements and between these and three traditional topology measurements, namely the degree, clustering and betweenness centrality. The Pearson correlation values, organized as a matrix, obtained for the ER and WAX networks are shown in Figures 8(a) and (b), respectively. The results are given only for two models because the correlation matrix of the BA case are similar to those of the ER model, and the matrix of the GEO network are similar to the WAX case. The backbone symmetry for $h = 2, 3, 4$ and merged symmetry for $h = 2, 3$ show strong correlations among themselves for the ER model. This is a consequence of the high regularity of this model, where the same neighborhood patterns appear at different concentric levels. The WAX model shows less correlation between the symmetry measurements, which might be caused by the large variability of patterns characteristic of this model. Also, there is low correlation between the symmetry measurements and the traditional ones, which indicates that the new measurements defined in the current work provide complementary information about the network structure that is not contained in the traditional ones.

IV. REAL-WORLD NETWORKS

We also illustrate the potential of the proposed symmetries for characterizing the local structure of some real-world networks.

Figure 9 shows the concentric patterns of the worldwide airports network ($N = 2940$ and $\langle k \rangle \approx 21$) in which

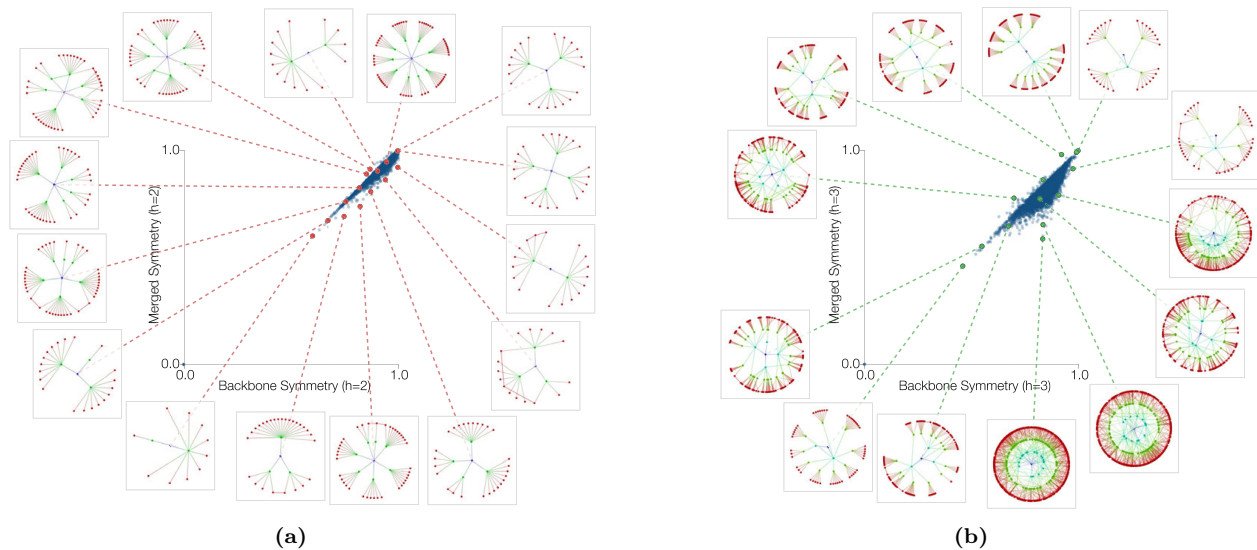


FIG. 3: Symmetries of the ER model for (a) $h = 2$ and (b) $h = 3$. The network has $N = 5 \times 10^3$ and average degree $\langle k \rangle = 6$.

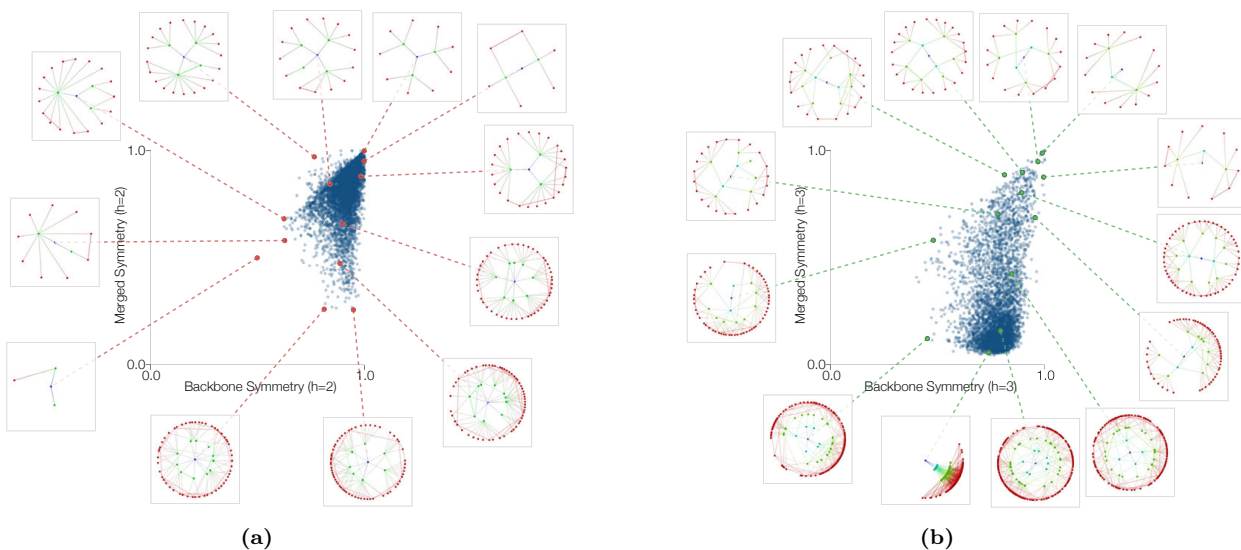


FIG. 4: Symmetries of the GEO model for (a) $h = 2$ and (b) $h = 3$. The network has $N = 5 \times 10^3$ and average degree $\langle k \rangle = 6$.

pairs of airports are connected if they share a route [26]. Interestingly, a whole different scenario is observed than those obtained for the random graphs examples. For instance, we see that the pairs of $\{Sb_i^{(h)}, Sm_i^{(h)}\}$ are much more distributed in the airport network than in all models. Analyzing the patterns in Figure 9, one interesting behavior is that a significant number of patterns have maximum values for one of the symmetries. For those with $S_b^{(2)} = 1$, it is possible to observe that they correspond to patterns centered at nodes with low degrees connected to hubs, yielding tree-like patterns. These nodes represent small airports connected to larger airports that

naturally have many connections. The patterns lying at $S_m^2 = 1$ correspond to highly clustered patterns, mainly composed by links at the same concentric level.

A similar behavior is shown in our next example, for the scientific areas of the Wikipedia network ($N = 45876$ and $\langle k \rangle \approx 5.8$). Here we consider that two pages in Wikipedia are connected if one is cited by the other, ignoring the direction of the citation. Again, as we can see in Figure 10, the dispersion in the symmetry space contrasts to the model cases as well as the previously observed patterns.

Remarkably, this contrast between real-world networks

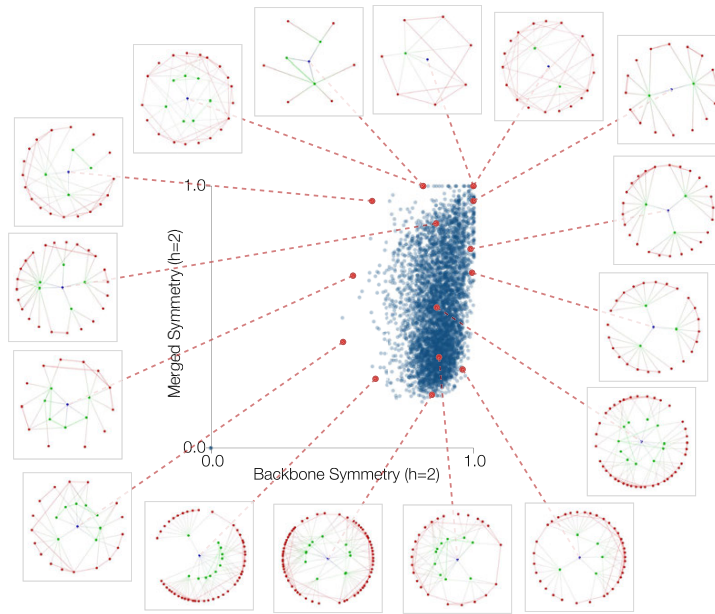


FIG. 5: Symmetries for a WAX network with $N = 5 \times 10^3$ and $\langle k \rangle = 6$.

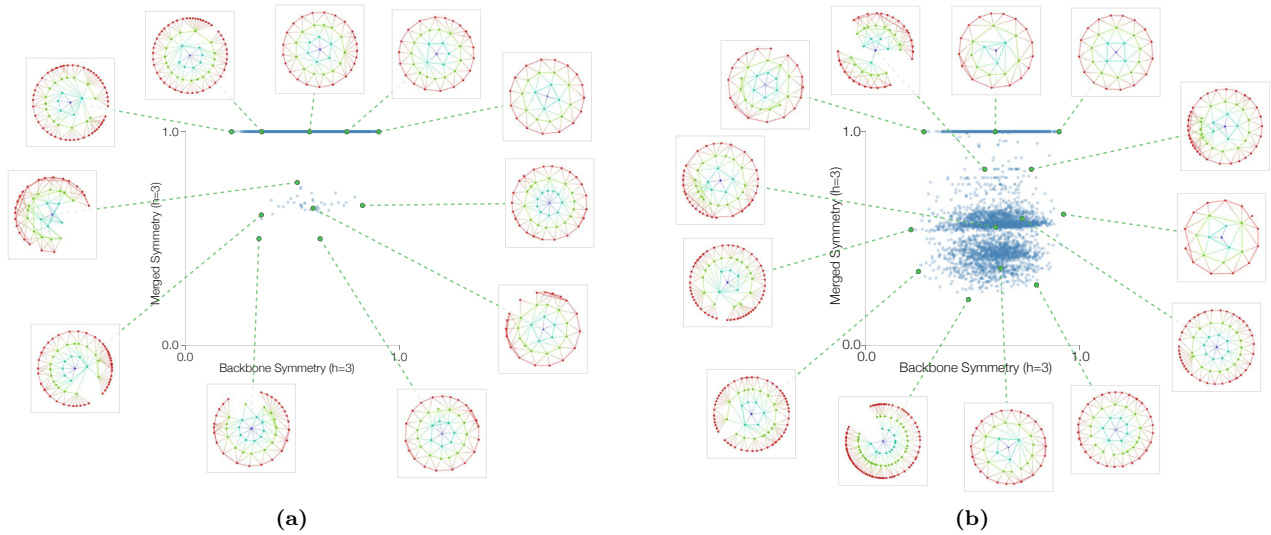


FIG. 6: Symmetries for $h = 3$ of the (a) VOR model and (b) RVOR model with probability 0.001 of random rewiring. Each network has $N = 5 \times 10^3$ and average degree $\langle k \rangle = 6$.

and random graph models is not observed for the real-spatial networks considered here, namely, the street networks of Oldenburg ($N = 14503$ and $\langle k \rangle \approx 2.8$) and San Joaquin [19] ($N = 2873$ and $\langle k \rangle \approx 2.6$), see Figure 11. In fact, similar distributions of measurements $\{Sb_i^{(h)}, Sm_i^{(h)}\}$ are observed for ER and random geographic models. It is also interesting to note that, although the two cities have different street planning

[20], both present similar dependence between $Sb_i^{(h)}$ and $Sm_i^{(h)}$.

Appendix A contains the scatterplots of the symmetry measurements colored according to the node degree. The street networks (shown in Figures 22 and 23) show the expected behavior of smaller symmetry values when the degree is increased, with some exceptions observed mainly for the airport (shown in Figure 20) and

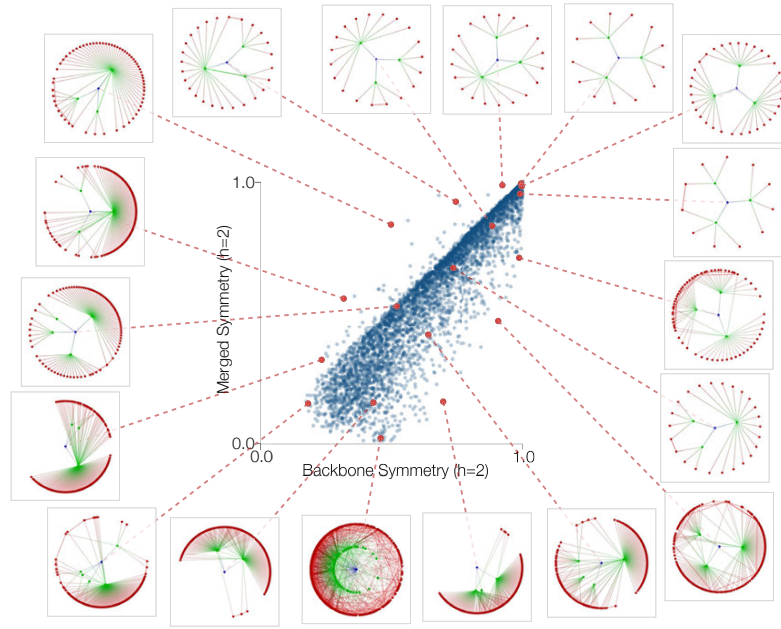


FIG. 7: Symmetries for $h = 2$ of a BA network with $N = 5 \times 10^3$ and $\langle k \rangle = 6$.

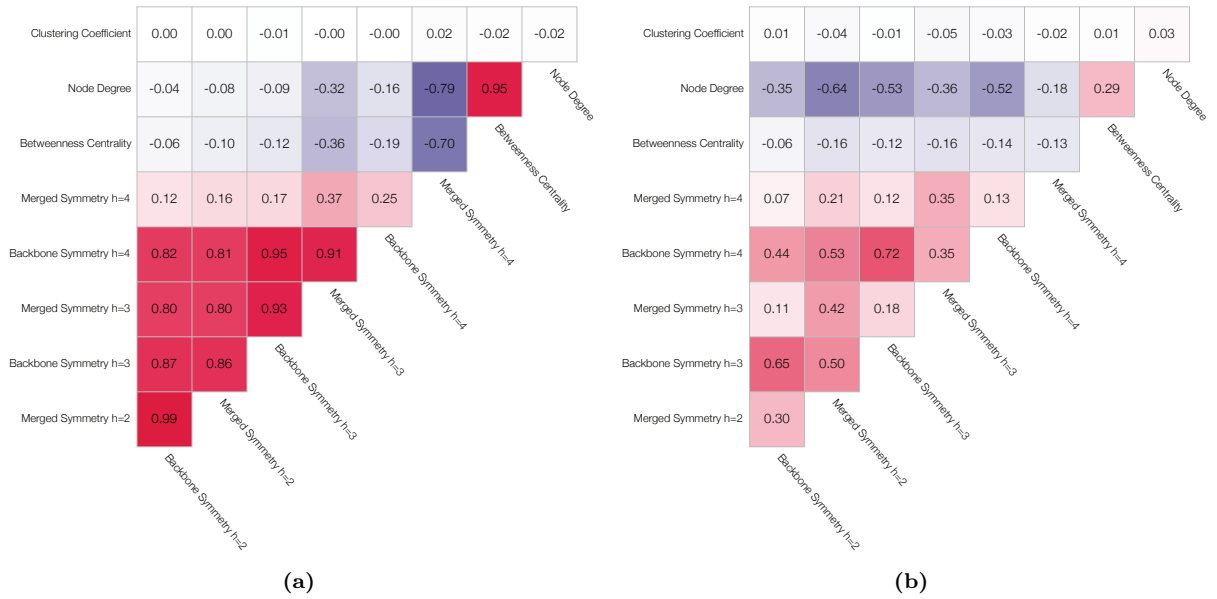


FIG. 8: Correlations between the symmetry measurements proposed here with some topological properties for (a) ER and (b) WAX model.

Wikipedia (shown in Figure 21) networks for $h = 4$.

The matrices with the Pearson correlation coefficients between the symmetry indices and three traditional topological measurements are shown in Figures 12(a) and (b) for the Oldenburg street network and the Wikipedia network, respectively. We note that the correlation matrix for San Joaquin is similar to the matrix calculated for

Oldenburg, and the correlations for the Wikipedia are similar to those in the airport network. The Oldenburg network, as expected, has large correlations between backbone and merged symmetries calculated at the same respective level. For both networks, the correlations between the symmetry measurements of distinct concentric levels are low, indicating that these measurements, taken

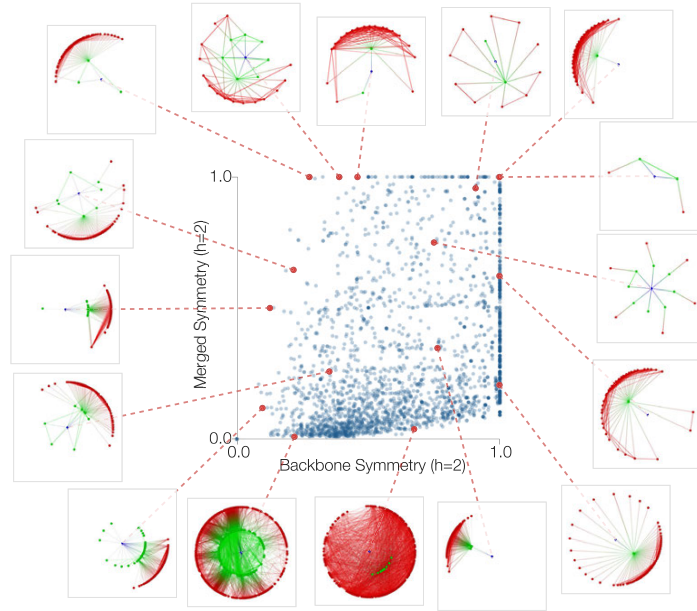


FIG. 9: Symmetries of the patterns for the airport network for $h = 2$.

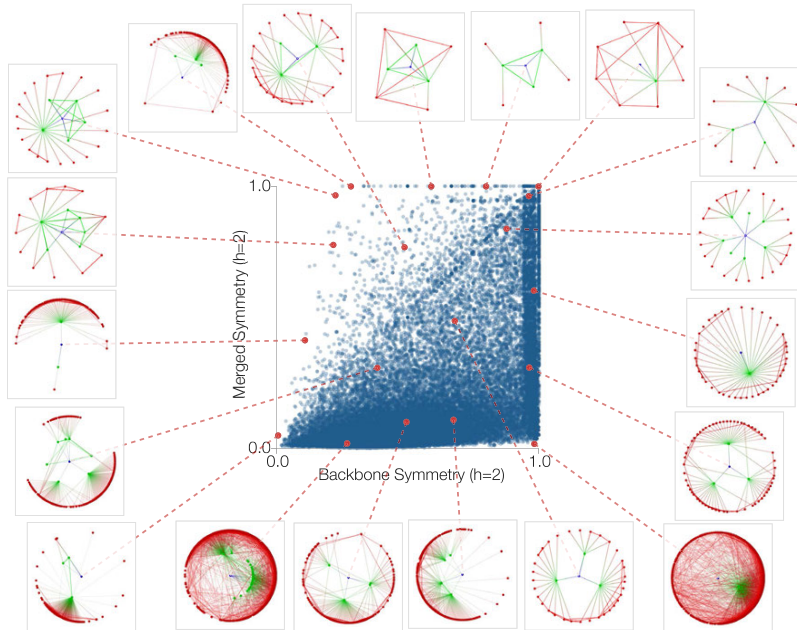


FIG. 10: Symmetries of the patterns for the scientific areas of the Wikipedia network for $h = 2$.

along the concentric levels, provide complementary information about the networks organization. Also, the correlations between the traditional measurements and the symmetry are very low.

V. STATISTICAL ANALYSIS

In order to obtain a concise comparison of the symmetry results obtained for all networks studied here, we apply the Principal Component Analysis [21] (PCA). Because the networks do not have the same number of ver-

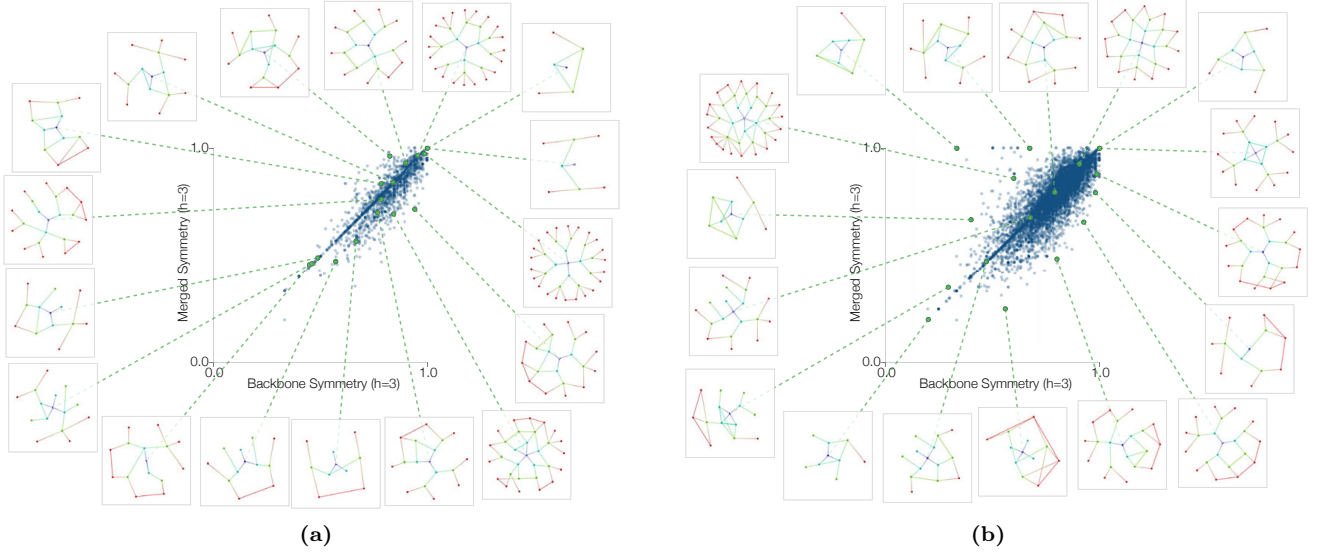


FIG. 11: Symmetries of the patterns for the Oldenburg (a) and San Joaquin (b) street networks for $h = 3$.

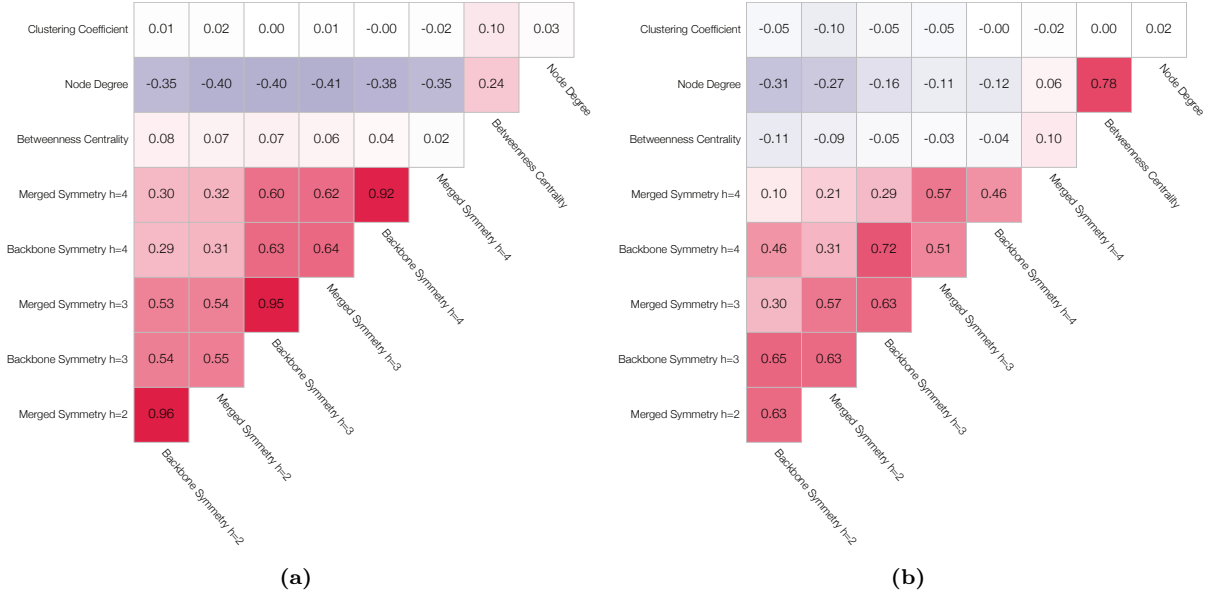


FIG. 12: Correlations between the symmetry measurements proposed here with some traditional topological properties for (a) the Oldenburg street network and (b) the Wikipedia citation network.

tices, we randomly selected 1000 nodes from each network and calculated the backbone and merged symmetries for $h = 2, 3$ and 4, this defines a 6-dimensional space containing all the selected nodes. The PCA is applied to this data and the first two components are retained, the result is shown in Figure 13(a). The PCA in Figure 13(a) encompasses most of the main results of this paper and highlights the relationships between the symmetric features of the considered networks. The two first PCA

axes have been verified to account for $\approx 86\%$ of the total variance. The component $PCA1$ corresponds to a balanced linear combination of all symmetry measurements, i.e. $PCA1 = 0.37Sb_i^{(2)} + 0.43Sm_i^{(2)} + 0.44Sb_i^{(3)} + 0.43Sm_i^{(3)} + 0.43Sb_i^{(4)} + 0.34Sm_i^{(4)}$. Therefore, higher values of $PCA1$ reflect higher symmetries. The Wikipedia, airports and BA networks present small $PCA1$ values (i.e. low symmetry), possibly reflecting their power law nature. GEO and WAX models presented little overlap

between themselves even though they share a geographical nature. This might be caused by the existence of long-range connections present in the WAX model, which are not allowed in the GEO networks. Both street networks presents great overlap in the PCA space and, along *PCA1*, they are closer to the ER model than to the geographical models. At the same time, the RVOR network presented an even larger overlap with the two cities.

In order to compare the results obtained using the symmetry measurements, we also applied the PCA considering several more traditional concentric characteristics [22] (e.g. concentric degree, clustering). The result is shown in Figure 13(b). By comparing the two PCA projections, it becomes clear that the symmetry measurements provide a more discriminative representation of the several considered networks, reflected in less overlap between clusters allied to wider distributions of nodes within the clusters associated to each network. The relatively small overlaps between some of the networks in Figure 13(a), such as between ER and the street networks, are indeed expected. A good deal of such remarkable properties can be understood to be related to the insensitivity of the symmetry measurements to the node degree, which otherwise implies in widely different sizes of clusters (see Figure 13(b)).

The spatial dispersion of the node symmetry measurements, quantified in terms of the trace of the respective covariance matrix, obtained for the several networks considered in this article, are given in Table I respectively to the concentric levels $h = 2, 3$, and 4.

In general, the PCA provides an important overview of the symmetry measurements. In addition, the *PCA1* axis retains 71% of their variance, this allow us to rank the networks in terms of an overall symmetry value, i.e. *PCA1*. The most symmetric networks are those of streets, followed by the ER model and the two spatial models. On the other hand, Wikipedia, airports and BA models are the more asymmetrical networks and also presenting the higher dispersion values for $h = 2$ (please see Table I). Such ordering along *PCA1* tends to reflect the regularity/simplicity of the original networks, a possibility that needs to be further investigated.

VI. CONCLUSIONS

Complex networks can be studied at different topological scales: local-scale characterized by the connectivity between neighbors of a node, intermediate-scale usually associated to communities; and global-scale concerning the overall structure of the network. While several methods have been developed for the characterization of global-scale symmetries in networks, mostly based on automorphism [1, 3], it is also interesting to develop concepts and methods capable of quantifying the symmetry more locally, e.g. around a given neighborhood of a node.

The concept of symmetry developed in the current article is associated to the regularity of the transition prob-

abilities of a concentric random walk. Since the calculations are always done using a single node as a reference, we can relate the concept of topological symmetry with our visual perception of symmetry. This relationship is particularly noticeable for the Erdős-Renyi model (ER). Since connections inside the same concentric levels are uncommon for the ER network, giving rise to a tree-like organization, the topological symmetry is mainly determined by the balance of connections along tree branches. This property also allows for a clear visualization of the topological symmetry.

The Barabási Albert (BA) model provides a nice contrast to the ER model, since it is highly probable that one or more hubs are accessed after one or two steps from the reference node. This property implies a strong unbalance on the transition probabilities of the concentric random walk, since nodes reached after passing through the hub are accessed with much lower probability than other nodes on the same concentric level that are not associated with hubs. Another interesting network model to be investigated is the spatial model. Since the nodes in these networks have a well-defined position influencing the connectivity of patterns, it is interesting to quantify how this influence translates to topological symmetry.

Regarding the real-world networks, it is interesting that the airport and Wikipedia showed a larger range of symmetry values than any network model. This might happen because the connectivity patterns of the nodes do not follow single rules as in the models, in the sense that they present a hybrid topology. For the airport networks, different countries or states have specific demands (e.g. passenger flow). In the Wikipedia, each subject (i.e., mathematics, biology, etc) tends to present specific citation patterns [23]. Still, the topological patterns are more symmetric than those observed in the models, which is confirmed by higher values of backbone and merged symmetry. This is probably a consequence of the adjacency constraints implied by planarity that need to be followed in city planning, such as in Voronoi networks [16]. Although the GEO network share many similar characteristics with the street networks, they are not specifically made to be navigable.

As developed in this work, the symmetry measurement was found to capture many distinct concentric patterns of connectivity. A natural extension of our analysis is to verify which of these patterns occur more often than it would be expected by chance on real-world networks. Therefore, by analyzing the density of points in the symmetry space we can identify motifs in the network structure. It would be important to verify how many distinct patterns can be associated to the same pair of symmetry values. Another additional development is to identify typical symmetry patterns specific to distinct regions of the real-world networks. For example, would a given region of the airport network present some intrinsic organization? Or, would given areas of Wikipedia exhibit typical symmetry patterns?

The symmetry of a network can also influence how a

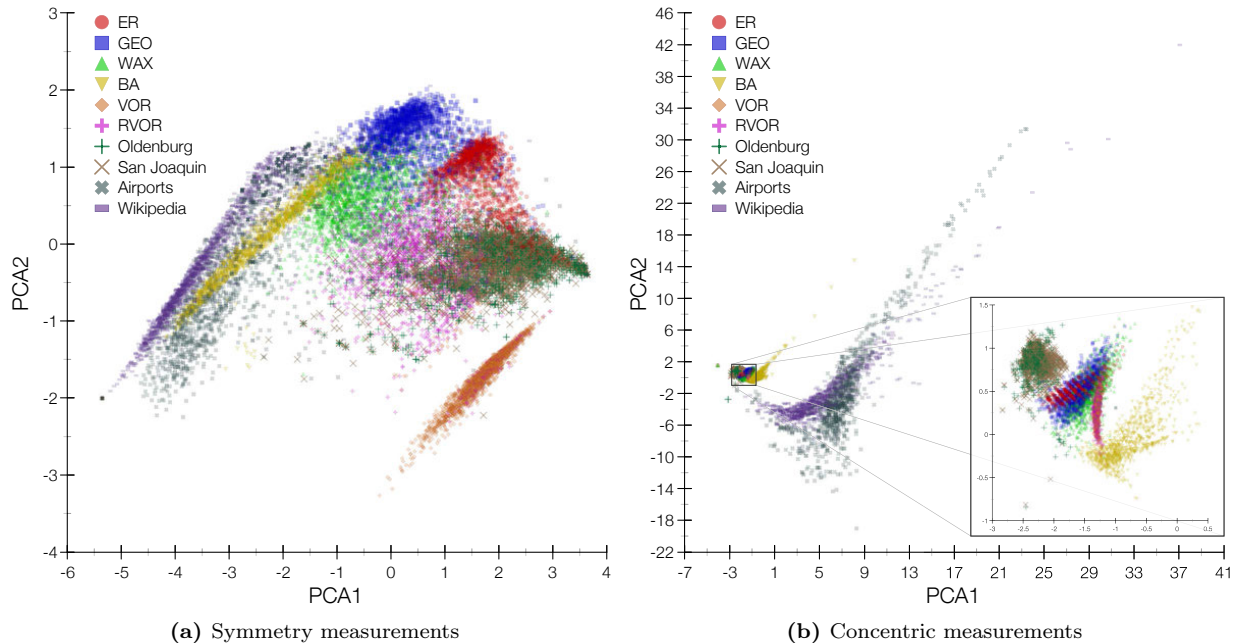


FIG. 13: PCAs obtained from the standardized backbone and merged symmetries from level $h = 2$ to $h = 4$ (a), and from concentric measurements [22] considering the same range of levels (b). Because the networks present distinct number of nodes, only 1000 nodes randomly sampled from each network are considered for the calculation.

TABLE I: Trace of the covariance matrix calculated for the backbone and merged symmetry values at each concentric level.

Concentric Level (h)	ER	GEO	WAX	Voronoi	Voronoi (Rewired)	BA	Oldenburg	San Joaquin	Airports	Wikipedia
2	0.010	0.020	0.044	0.005	0.039	0.112	0.023	0.021	0.182	0.144
3	0.011	0.052	0.034	0.013	0.069	0.021	0.038	0.038	0.081	0.033
4	0.067	0.014	0.022	0.019	0.050	0.005	0.039	0.039	0.040	0.007
All	0.088	0.086	0.100	0.037	0.158	0.138	0.100	0.098	0.303	0.184

disease propagate over the network. Diffusion and disease dynamics are of particular interest since it is possible to analyze how the number of symmetric patterns in the network impacts the speed of a dynamics propagation. This idea is related to some previous results showing that degree heterogeneity can facilitate disease propagation on networks [24, 25].

Acknowledgements

F. N. Silva acknowledges CAPES. C. H. Comin thanks FAPESP (Grant No. 11/22639-8) for financial support. T. K. D. M. Peron acknowledges FAPESP (Grant no.

2012/22160-7) for support. F. A. Rodrigues acknowledges CNPq (grant 305940/2010-4), FAPESP (grant 2011/50761-2 and 2013/26416-9) and NAP eScience - PRP - USP for financial support. L. da F. Costa thanks CNPq (Grant no. 307333/2013-2) and NAP-PRP-USP for support. This work has been supported also by FAPESP grants 12/50986-7 and 11/50761-2.

Appendix A: Correlation between symmetry and degree

[1] C. Godsil and G. F. Royle, in *Algebraic Graph Theory* (Springer, 2001).

[2] R. Scapellato and J. Lauri, London Math. Soc., Student Text **54** (2003).

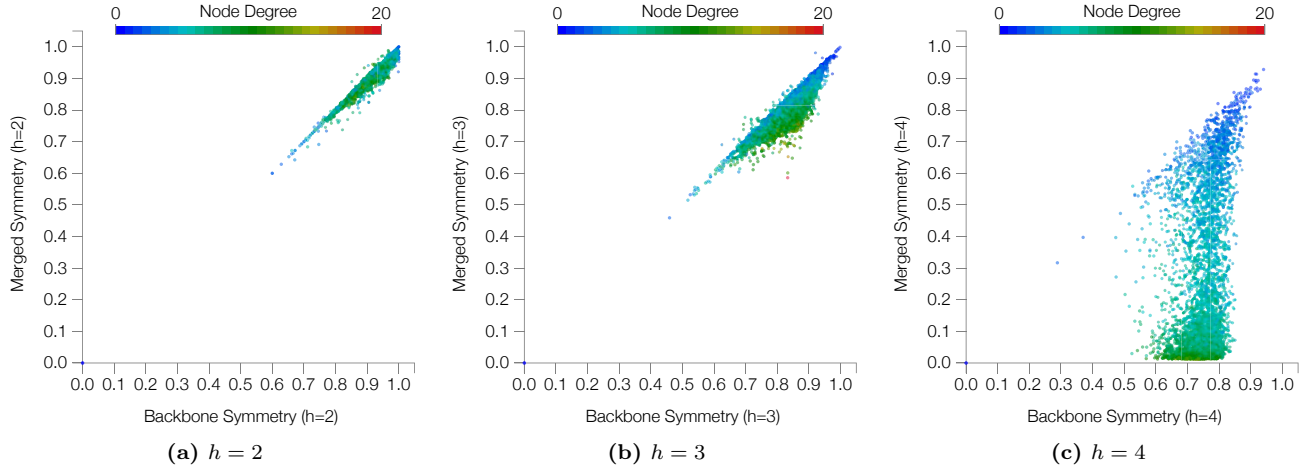


FIG. 14: Scatterplots of backbone vs merged symmetry measurements for the ER network considering concentric levels $h = 2, 3$ and 4. The points are colored according to the degree of the respective node.

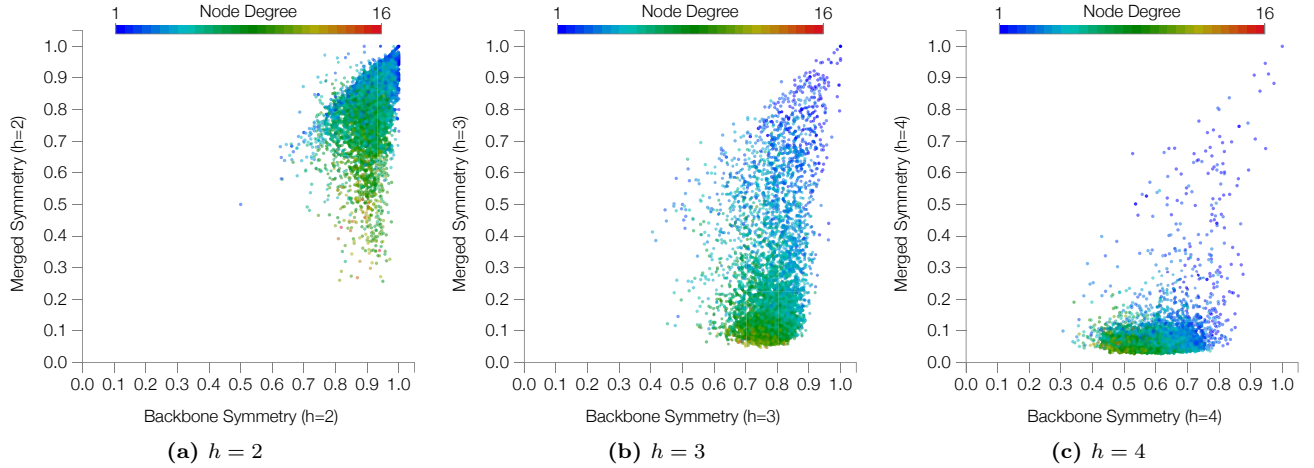


FIG. 15: Scatterplots of backbone vs merged symmetry measurements for the GEO network considering concentric levels $h = 2, 3$ and 4. The points are colored according to the degree of the respective node.

- [3] N. Biggs, *Algebraic Graph Theory* (Cambridge University Press, 1994).
- [4] L. W. Beineke and R. J. Wilson, *Topics in Algebraic Graph Theory*, vol. 102 (Cambridge University Press, 2004).
- [5] Y. Xiao, M. Xiong, W. Wang, and H. Wang, *Physical Review E* **77**, 066108 (2008).
- [6] P. Holme, *Physical Review E* **74**, 036107 (2006).
- [7] B. D. MacArthur, R. J. Sánchez-García, and J. W. Anderson, *Discrete Applied Mathematics* **156**, 3525 (2008).
- [8] M. P. Viana, J. L. Batista, and L. da F. Costa, *Physical Review E* **85**, 036105 (2012).
- [9] B. A. N. Travençolo, M. P. Viana, and L. d. F. Costa, *New Journal of Physics* **11**, 063019 (2009).
- [10] B. Travençolo and L. da F. Costa, *Physics Letters A* **373**, 89 (2008).
- [11] L. da F. Costa and F. A. Rodrigues, *Europhysics Letters* **85**, 48001 (2009).
- [12] L. da F. Costa, M. A. R. Tognetti, and F. N. Silva, *Physica A* **387**, 6201 (2008).
- [13] M. Newman, *Networks: An Introduction* (Oxford University Press, 2010).
- [14] J. Dall and M. Christensen, *Physical Review E* **66**, 016121 (2002).
- [15] B. M. Waxman, *Selected Areas in Communications, IEEE Journal on* **6**, 1617 (1988).
- [16] M. Barthélemy, *Physics Reports* **499**, 1 (2011).
- [17] E. Estrada, *The structure of complex networks: theory and applications* (Oxford University Press, New York, 2012), ISBN 978-0-19-959175-6.
- [18] L. da F. Costa, *International Journal of Modern Physics C* **15**, 175 (2004).
- [19] T. Brinkhoff, *Geoinformatica* **6**, 153 (2002).
- [20] L. Lacasa and J. Gómez-Gardeñes, *Phys. Rev. Lett.* **110**,

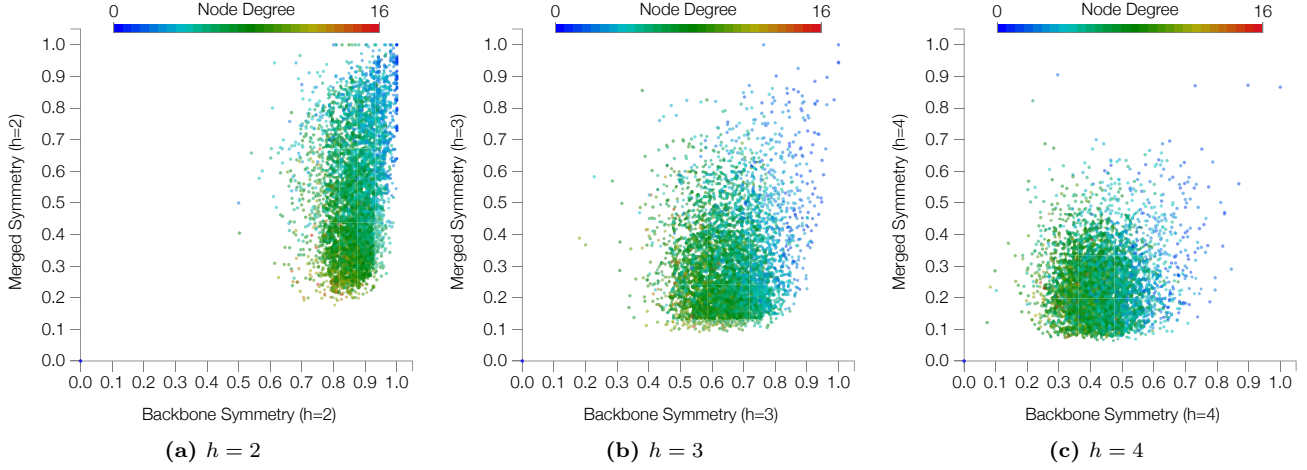


FIG. 16: Scatterplots of backbone vs merged symmetry measurements for the WAX network considering concentric levels $h = 2, 3$ and 4 . The points are colored according to the degree of the respective node.

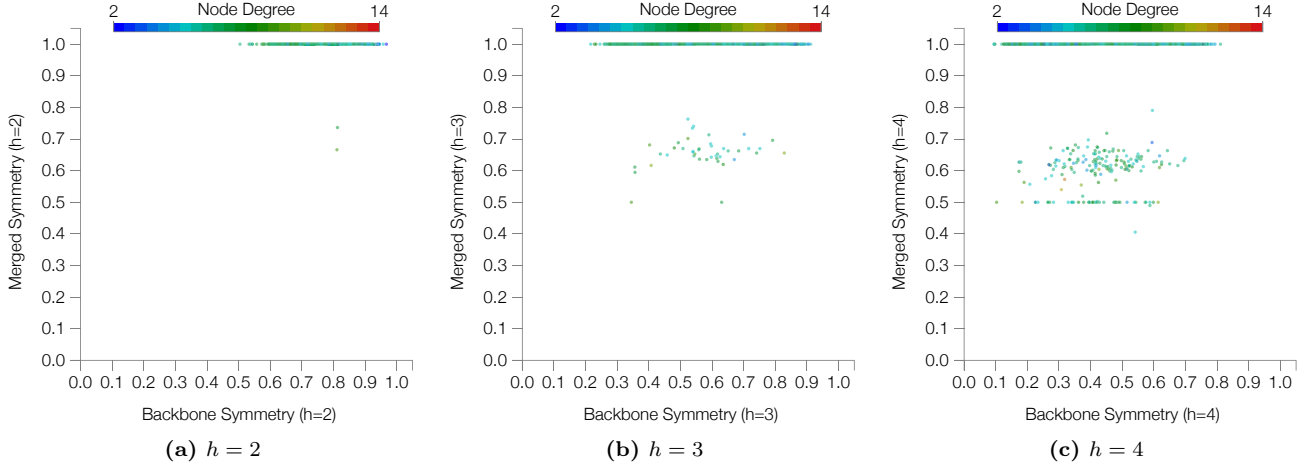


FIG. 17: Scatterplots of backbone vs merged symmetry measurements for the VOR network considering concentric levels $h = 2, 3$ and 4 . The points are colored according to the degree of the respective node.

168703 (2013).

[21] I. T. Jolliffe, *Principal component analysis* (Springer, 2002).

[22] L. da. F. Costa and F. N. Silva, *J Stat Phys* **125**, 845 (2006).

[23] F. Silva, M. Viana, B. Travençolo, and L. da F. Costa, *Journal of Informetrics* **5**, 431 (2011).

[24] R. Pastor-Satorras and A. Vespignani, *Physical Review Letters* **86**, 3200 (2001).

[25] F. J. Pérez-Reche, S. N. Taraskin, W. Otten, M. P. Viana, L. da F. Costa, and C. A. Gilligan, *Physical Review Letters* **109**, 098102 (2012).

[26] The airport and route data were obtained from <http://sourceforge.net/p/openflights/code/HEAD/tree/openflights/data/>

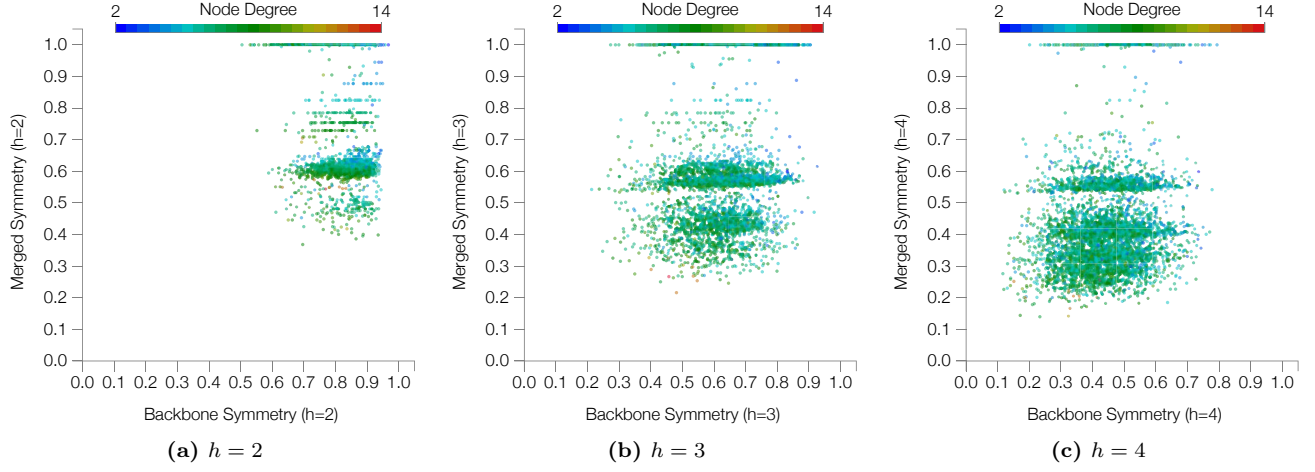


FIG. 18: Scatterplots of backbone vs merged symmetry measurements for the RVOR network considering concentric levels $h = 2, 3$ and 4 . The points are colored according to the degree of the respective node.

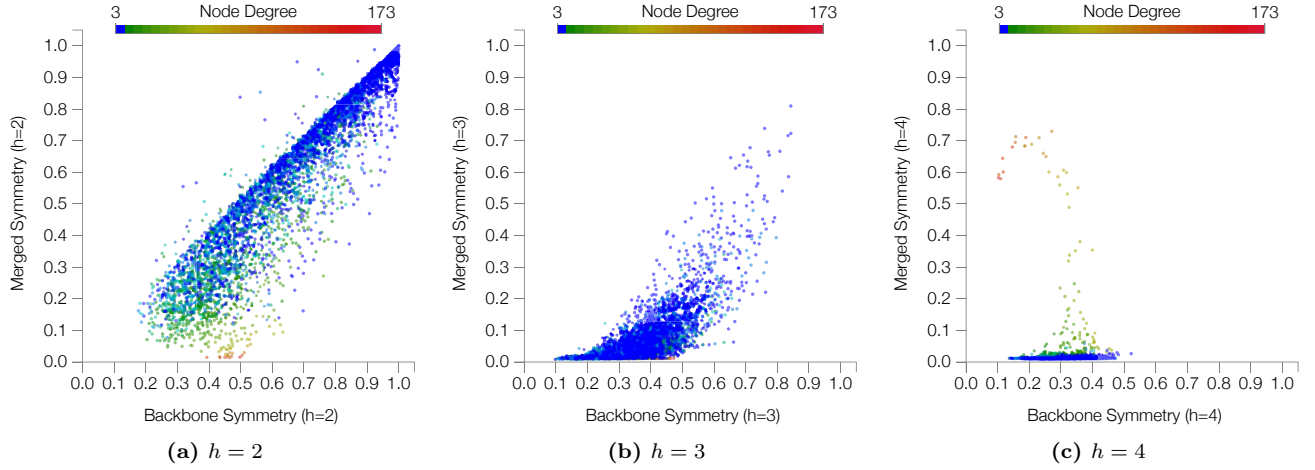


FIG. 19: Scatterplots of backbone vs merged symmetry measurements for the BA network considering concentric levels $h = 2, 3$ and 4 . The points are colored according to the degree of the respective node.

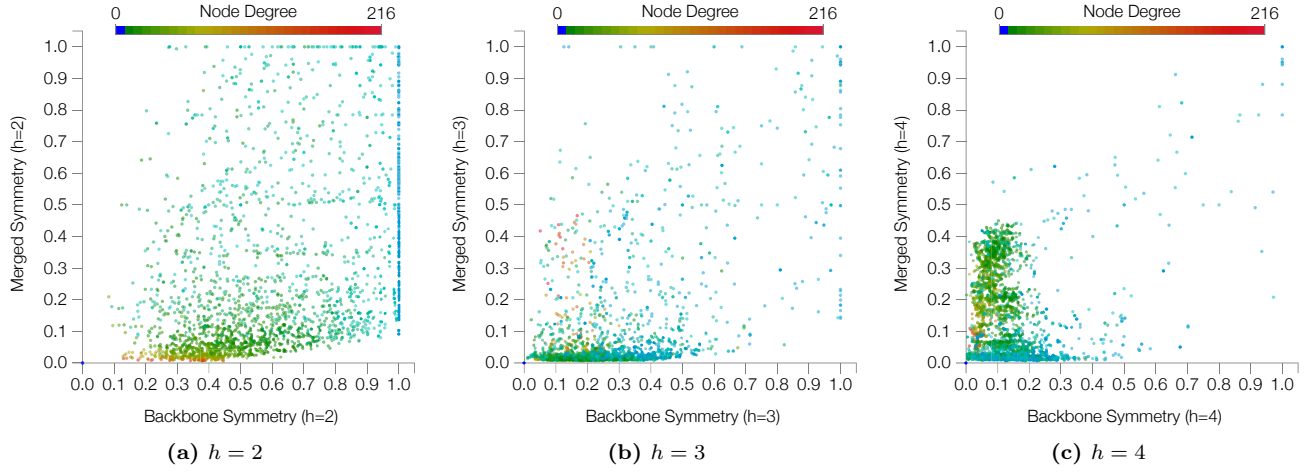


FIG. 20: Scatterplots of backbone vs merged symmetry measurements for the airport network considering concentric levels $h = 2, 3$ and 4. The points are colored according to the degree of the respective node.

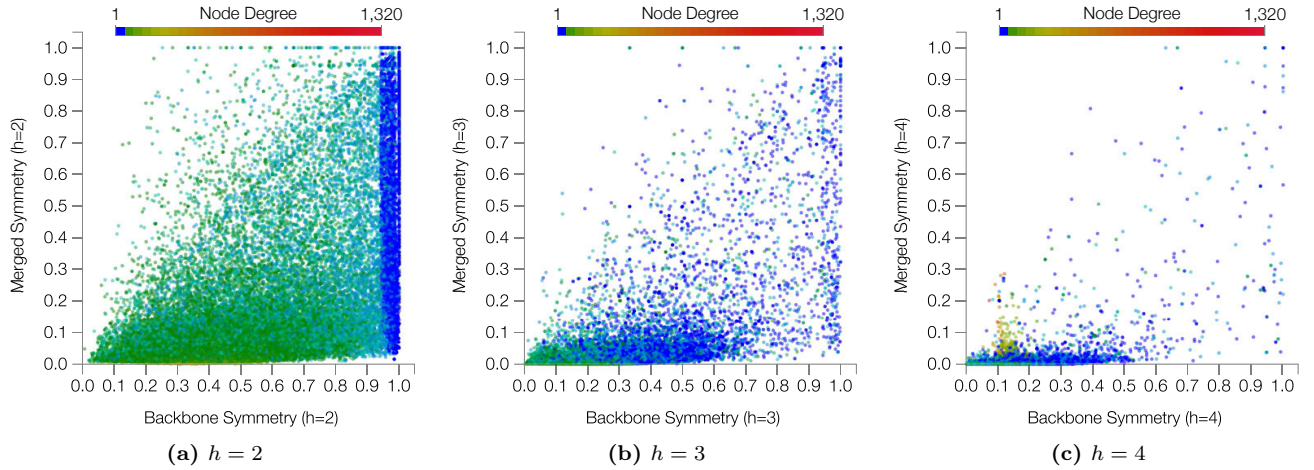


FIG. 21: Scatterplots of backbone vs merged symmetry measurements for the Wikipedia network considering concentric levels $h = 2, 3$ and 4. The points are colored according to the degree of the respective node.

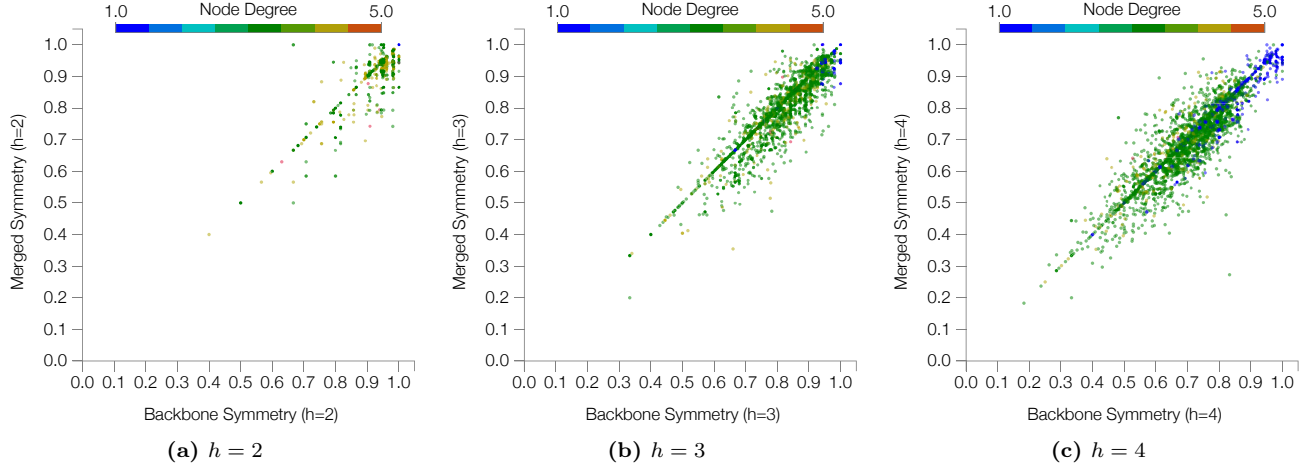


FIG. 22: Scatterplots of backbone vs merged symmetry measurements for the Oldenburg City network considering concentric levels $h = 2, 3$ and 4 . The points are colored according to the degree of the respective node.

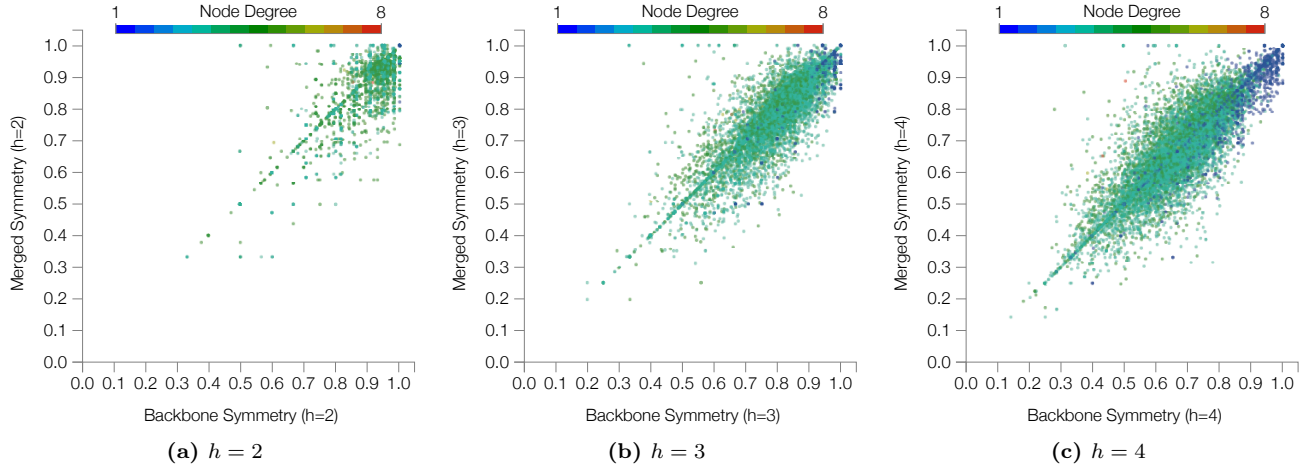


FIG. 23: Scatterplots of backbone vs merged symmetry measurements for the San Joaquin County network considering concentric levels $h = 2, 3$ and 4 . The points are colored according to the degree of the respective node.